Rapid #: -10840772

CROSS REF ID: **10733**

LENDER: **CSL :: Main Library**

BORROWER: **NJI :: Main Library**

TYPE:	Article CC:CCL
JOURNAL TITLE:	Cell motility and the cytoskeleton
USER JOURNAL TITLE:	Cell motility and the cytoskeleton.
ARTICLE TITLE:	Buckling of a single microtubule by optical trapping forces: Direct measurement of microtubule rigidity
ARTICLE AUTHOR:	Kurachi, M.,
VOLUME:	30
ISSUE:	3
MONTH:	
YEAR:	1995
PAGES:	221 - 228
ISSN:	0886-1544
OCLC #:	12848217

Processed by RapidX: 7/29/2016 7:12:12 AM

Cell Motility and the Cytoskeleton 30:221–228 (1995)

Buckling of a Single Microtubule by Optical Trapping Forces: Direct Measurement of Microtubule Rigidity

Masashi Kurachi, Masayuki Hoshi, and Hideo Tashiro

Laboratory of Photo-Biology, Photodynamics Research Center, The Institute of Physical and Chemical Research (RIKEN), Miyagi, Japan

As major determinants of cell shape and polarity, microtubules are required to have suitable rigidity. However, our knowledge of the mechanical properties of microtubules is far from satisfactory. We report here a new method of measuring the flexural rigidity of a single microtubule by direct buckling using the optical trapping technique. Microtubule buckling was induced by applying a small longitudinal compressing force through an optically trapped microsphere that was firmly attached to the microtubule. Three ways of estimating the flexural rigidity of a continuous slender rod, one from the observed critical load of buckling and two from deflected lengths and angles of bending, yielded values which agreed well when applied to the analysis of buckling microtubules. Unexpectedly, we found that the rigidity was not constant as expected but was dependent on microtubule length. This length dependency explains the discrepancies among reported values of microtubule flexural rigidity measured by different methods. Comparing microtubules of identical lengths, microtubules assembled with brain-derived associated proteins (4×10^{-23} Nm^2 at around 10 μm in length) were four times more rigid than those assembled from purified tubulin and stabilized with taxol (1×10^{-23} Nm^2).

Key words: microtubules, flexural rigidity, optical trapping, microtubule-associated proteins, taxol

INTRODUCTION

Microtubules have a cylindrical tube structure with an outer diameter of 25 nm, and are composed of α- and β-tubulin heterodimer subunits arranged into 13 protofilaments. It has been suggested that the stiffness of microtubules, possibly controlled by microtubule-associated proteins (MAPs: MAP2 and tau in particular), plays a critical role in the establishment of neuronal morphology [Edson et al., 1993; Matus, 1994]. The bending stiffness of microtubules has been calculated from quantitative analyses of the spontaneously bending curvatures of filaments [Mizushima-Sugano et al., 1983] or the thermal fluctuations of curvatures [Gittes et al., 1993]. The flexural rigidity obtained in these two experiments, however, showed a difference of two orders of magnitude: 4.5×10^{-25} nm^2 for MAPs-stabilized microtubules in the former and 2.2×10^{-23} nm^2 for taxol-stabilized microtubules in the latter. Contrary to these values, it was clearly shown that MAP2-containing microtubules were more resistant to bending than taxol-stabilized polymers in a flow of liquid medium [Dye et al., 1993]. Furthermore, Venier et al. [1994] recently obtained higher rigidity values for GDP microtubules compared with taxol-stabilized microtubules both by hydrodynamic bending analysis and thermal fluctuation analysis. Values obtained by these two methods agreed reasonably well but were an order of magnitude different from that of taxol-stabilized microtubules reported by Gittes et al. [1993].

Received July 11, 1994; accepted November 4, 1994.

Address reprint requests to Masashi Kurachi, Laboratory of Photo-Biology, Photodynamics Research Center, The Institute of Physical and Chemical Research (RIKEN), 19-1399 Koeji, Nagamachi, Aoba-ku, Semdai, Miyagi 980, Japan.

Dr. Masayuki Hoshi's current address is Department of Basic Science, Faculty of Science and Technology, Ishinomaki Sensyu University, Ishinomaki, Miyagi 986, Japan.

In addition to such discrepancies in absolute values, there remains a fundamental question of whether a limit exists in the application of linear macroscopic elasticity theory to microtubules with nanometer-scale subunit structure. In order to clarify this point, we analyzed buckling of a single microtubule, which was directly controlled by well-defined point forces. This was made possible by the recently developed optical trapping techniques [Askin and Dziedzie, 1987], which enable us to manipulate single microspheres with forces as large as several tens of pico-newtons. Using forces loaded through microspheres attached to a microtubule, buckling tests can be performed on a single microtubule in a manner analogous to buckling tests on macroscopic rods.

MATERIALS AND METHODS

Preparation of Microtubules

Microtubule protein was prepared from bovine brain by three cycles of temperature-dependent assembly and disassembly [Shelanski et al., 1973]. Purified tubulin was obtained by phosphocellose column chromatography [Sloboda et al., 1976] of microtubule proteins. Protein concentrations were determined by the Bradford method using a Bio-Rad protein assay kit [Bradford, 1976]. MAP-stabilized microtubules were polymerized by incubating 0.35–0.6 mg/ml of microtubule-proteins in Pipes buffer (90 mM Pipes, 1.8 mM EGTA, 0.9 mM $MgCl_2$, and 2.7 mM GTP, pH 6.9) at 37°C for 30 min. Taxol-stabilized microtubules were polymerized from 0.3 mg/ml of purified tubulin in Pipes buffer containing 10 μM taxol and were diluted 20 times with the same solution. As possible adhesive microspheres for microtubules, we examined polystyrene microsphere (0.3–1.0 μm in diameter) and glass microsphere (1.6 μm in diameter, Duke Scientific Corp., Palo Alto, CA), both of which were coated with poly-L-lysine (Sigma, St. Louis, MO). Glass microspheres with a diameter of 1.6 μm, the smallest diameter commercially available, were adopted in the following buckling experiment, as only glass microspheres were found to adhere firmly to microtubules. One microliter of Pipes buffer containing glass microspheres coated with poly-L-lysine was then added to 20 μl of the sample solution containing polymerized microtubules, 15 μl was pipetted onto a cleaned microscope slide glass, and a cleaned coverglass was placed on top. The separation between the inner glass surfaces of the glasses was kept to about 20 μm using aluminum foil spacers. Edges of the coverglass were sealed with valap (beeswax:lanolin:petrolatum, 1:1:1, by wt). A prepared sample was set on a microscope heating stage, which was maintained at 37°C.

Video-Enhanced DIC Microscopy With Optical Tweezers

Figure 1 presents a schematic diagram of the optical system for the measurement. Microtubules and glass microspheres were observed under a differential interference contrast microscope (Carl Zeiss, Axiovert 135 TV, Germany), equipped with a Plan Apochromat 63× oil-immersion objective lens (numerical aperture = 1.4), an oil-immersion condenser lens for high-magnification objectives, and a 100-W halogen lamp. Images were detected with a Newvicon camera (Hamamatsu, C2400-07, Hamamatsu, Japan), enhanced with an image processor (Hamamatsu, DVS-1000, Hamamatsu, Japan), and recorded with a Super-VHS video cassette recorder (JVC, BR-S822, Yokohama, Japan). A video printer (Sony, UP-860, Tokyo, Japan) was used for video prints of taped images. A linearly polarized laser beam in the TEM_{00} mode from a krypton ion laser (LASER IONICS Inc., Model 1401-2K, Orlando, FL) whose wavelength was 647.1 nm was introduced into the epifluorescence port of the microscope with the aid of collimating lenses and galvano mirrors (General Scanning Inc., Watertown, MA). The trapping laser beam was manipulated in two dimensions over the field of view (about 50 μm × 35 μm) using the galvano mirrors. Rotation of a Glan-laser polarizer or a half-wave plate inserted in front of it allowed continuous attenuation of the laser beam during experiments. The laser power incident on the microscope was measured by a thermal detector (OPHIR OPTRONICS Inc., Model 10A, Jerusalem, Israel). The trapping force of the optical tweezers was calibrated by applying the Stokes drag law for a single microsphere by holding it stationary against a relative flow made by translating the microscope stage at a constant speed. The results of calibration in the solution containing tubulin below the critical concentration for polymerization showed the trapping force to be proportional to the laser power with a relationship of 0.3 ± 0.05 pN/mW in the range of 0.1 to 8 pN.

Analysis of Deflection of an Elastic Rod

In order to evaluate the flexural rigidity, we apply deflected curvature analysis of a continuous slender rod to a single microtubule. When the compressing force applied at both ends exceeds the critical load, the slender elastic rod starts buckling. The shape of the deflected rod follows a curve known as "elastica," which was first analyzed by Euler and also by Lagrange [Timoshenko and Gere, 1961; Feynman et al., 1964].

Figure 2 shows a highly deflected state with compressing forces of P at both hinged ends. This state is directly analyzed by applying the one-fixed and one-free end model described by Timoshenko and Gere, in refer-

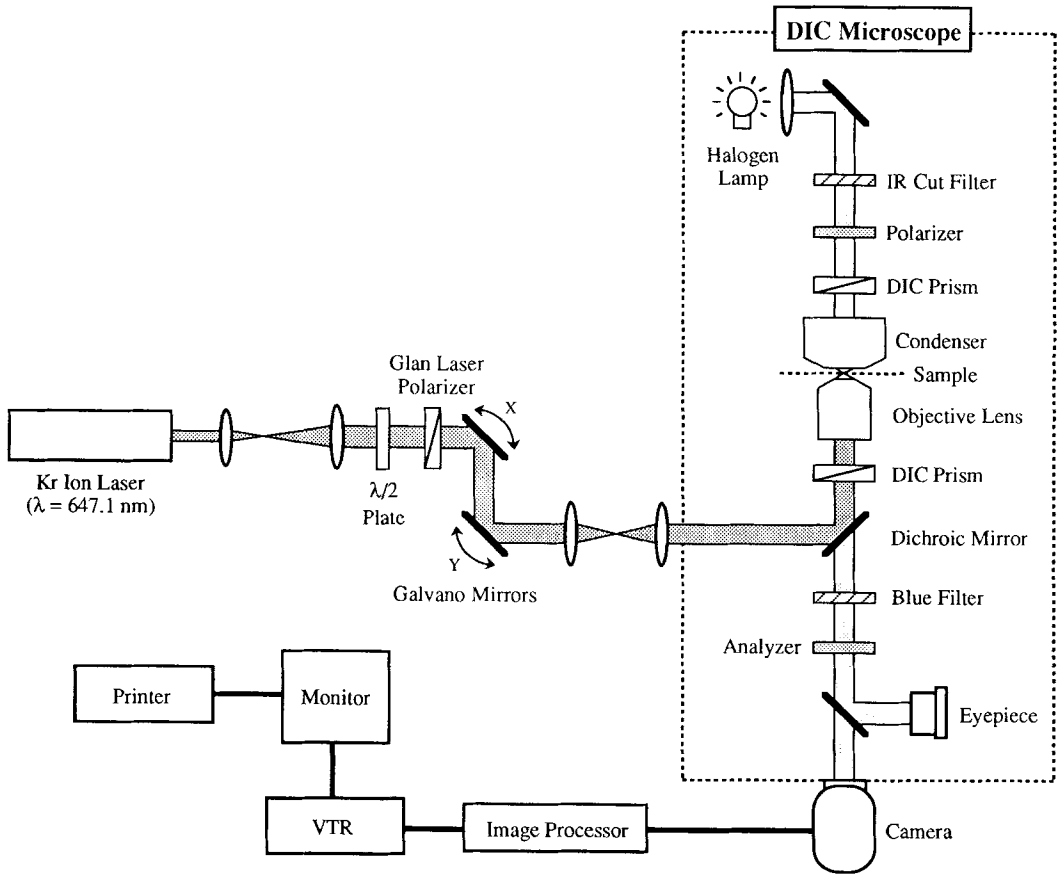

Fig. 1. Schematic diagram of the video-enhanced DIC microscope with optical tweezers. The laser power is controlled by rotating the Glan-laser polarizer or the half-wave plate in front of it.

ence to the rod, which is bent with a fixed end at the center (x_d, y_d) since the curvature is symmetric. For an elastic rod, the bending moment is equal to the product of the flexural rigidity and the curvature of bending, and the exact differential equation is written as

$$EI \frac{d\theta}{ds} = -Py \tag{1}$$

where EI is the flexural rigidity, E is Young's modulus, and I is the geometrical moment of inertia of cross section. Using the relation $dy = \sin\theta \cdot ds$, Eq. (1) is rewritten as

$$EI \frac{d^2\theta}{ds^2} = -P\sin\theta \tag{2}$$

Applying the boundary condition that $d\theta/ds = 0$ at $\theta = \alpha$, we obtain

$$L = \frac{2}{q}\int_0^{1/2} \frac{d\phi}{\sqrt{1 - p^2 \sin^2\phi}} = \frac{1}{q} K(p) \tag{3}$$

where $p = \sin(\alpha/2)$, $\sin(\theta/2) = p \cdot \sin\phi$, and $q^2 = P/EI$. The quantity $\sin\phi$ is chosen so that it varies from 0 to 1 when θ changes from 0 to α. The integral K(p) is known as a complete elliptic integral of the first kind.

Since the deflection is small at the beginning of buckling, Eq. (3) is rewritten as follows by neglecting the term $p^2 \cdot \sin^2\phi$.

$$L = \frac{4}{q}\int_0^{\pi/2} d\phi = \frac{\pi}{2q} = \frac{\pi}{2}\sqrt{\frac{EI}{P_{cr}}} \tag{4}$$

$$P_{cr} = \frac{\pi^2 EI}{L^2} \tag{5}$$

This relation is well known as Euler's equation and defines the critical load.

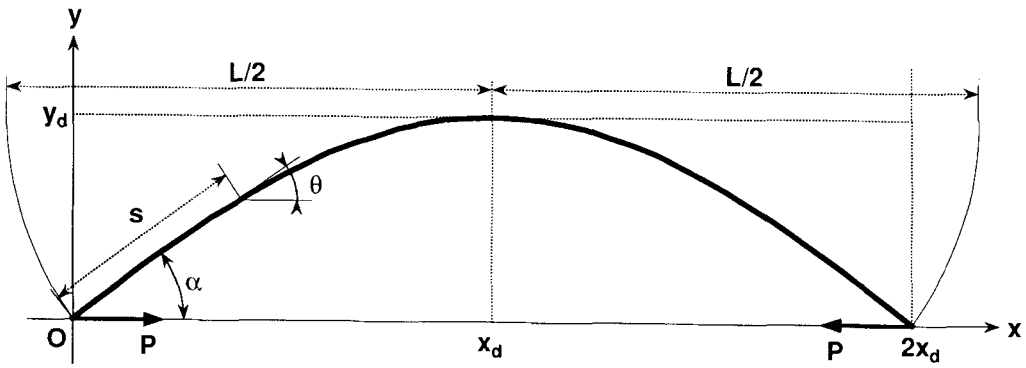

Fig. 2. Schematic representation of a deflected elastic rod.

Deflections y_d and x_d are obtained similarly as

$$y_d = \frac{2p}{q}\int_o^{\pi/2} \sin\phi \, d\phi = \frac{2p}{q} \tag{6}$$

$$x_d = \frac{2}{q}\int_0^{\pi/2} \sqrt{1 - p^2 \sin^2 \phi}\, d\phi - \frac{L}{2}$$

$$= \frac{2}{q} E(p) - \frac{L}{2} \tag{7}$$

where E(p) is a complete elliptic integral of the second kind.

Measurement of Flexural Rigidity

Using the analysis described above, there are three possible ways of determining the flexural rigidity EI from experimentally observable values (Fig. 3). One is to measure the critical load which directly leads to a value of EI through Eq. (5). The second is to measure deflected angle α under a load P. Since K(p) depends only on p, the deflected angle can be uniquely determined by EI according to Eq. (3) if L and P are given. The third is to measure the deflected length x together with L and P. Combining Eq. (3) with Eq. (7), we obtain

$$\frac{K(p)}{E(p)} = \frac{2}{1 + x/L} \tag{8}$$

If the deflected angle is below π/2 in the measurements, K(p)/E(p) is uniquely chosen from a numerical table to coincide with a measured value of x/L. Using this K(p), we can calculate EI according to the equation

$$EI = \frac{PL^2}{4K(p)^2} \tag{9}$$

Optical tweezers cannot directly trap a filamentous microtubule for individual compressive loading. For this reason, we must use microspheres stuck to the microtubules. Two glass microspheres coated with poly-L-lysine were successively trapped and transported near to a single microtubule in solution using optical tweezers. One microsphere was then moved and attached to the inner surface of the coverglass, while the other microsphere was moved with the optical tweezers so that a longitudinal compressing force was applied to the microtubule.

In practice, we used these three methods to determine microtubule rigidity. The critical load measurement is simple and straightforward, but the judgment of initiation of buckling was crucial under microscope observation. The measurement of deflected angles is also crucial because the tangent line of filament curvature at a microsphere is ambiguous. In order to avoid the ambiguity inherent in the above two methods, we primarily adopted the deflected length measurement. The deflected length, x, was measured as the closest distance attained by the two microspheres at the limit of bending when the constant force, P ($P > P_{cr}$), was applied to a microtubule. This closest distance is clearly measured from a video record because the moved microsphere escapes from the trap beyond this limit.

RESULTS

As shown in Figure 4, we found that a microtubule was easily deflected by applying several piconewtons of force to the optically trapped glass microsphere which was firmly attached to the microtubule. Buckling was initiated by moving the optically trapped microsphere on the left (Fig. 4b), starting from a spontaneously stretched state (Fig. 4a). The critical load with which the microtubule started bending was measured to be 1.5 pN. With increased trapping forces of 2.2 pN (Fig. 4c) and 2.9 pN (Fig. 4d), the microtubule was further buckled to the

limit where the trapping force was balanced with the recovery force of the microtubule. Beyond the bending limit, the microsphere escaped from the trap and the microtubule recovered to the initial stretched condition (Fig. 4e). The longitudinal compressing force was varied from 0.3 pN to 7.5 pN by changing the applied laser power from 1 mW to 25 mW. Within this range, no appreciable irradiation damage was recognized in the microtubule structure.

The critical loads were measured to be 1.0 to 3.0 pN for MAP-stabilized microtubules (L = 10 to 28 μm) and 0.4 to 0.7 pN for taxol-stabilized microtubules (L = 4 to 12 μm). The flexural rigidity was estimated to be (3.4 to 12.0) × 10^{-23} Nm^2 for MAP-stabilized microtubules and (0.13 to 0.86) × 10^{-23} Nm^2 for taxol-stabilized microtubules. These results are summarized in

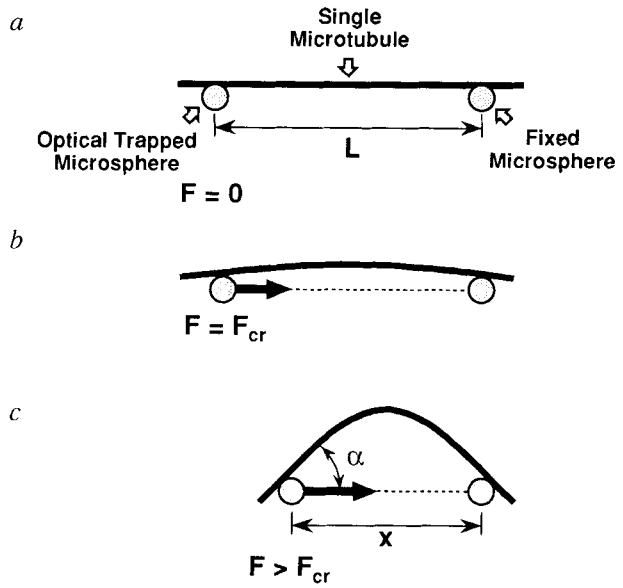

Fig. 3. Schematic diagrams of measurement of microtubule rigidity. **a:** A microtubule with two glass microspheres attached, one (on the right) is fixed to the glass surface, the other (on the left) is trapped by laser beam and can be moved. When no force is applied, the microtubule is straight. **b:** When longitudinal compressing force, P, reaches the critical force, P_{cr}, given by Euler's equation for small deflections (Eq. (5)), the microtubule is in unstable equilibrium and starts to bend. **c:** When applied force P exceeds P_{cr}, the bending of a microtubule follows the exact differential equation for large deflections. The relationship between P and L is given by Eq. (9). Deflected length, x, was measured as the minimum distance attained by the two microspheres at the limit of bending.

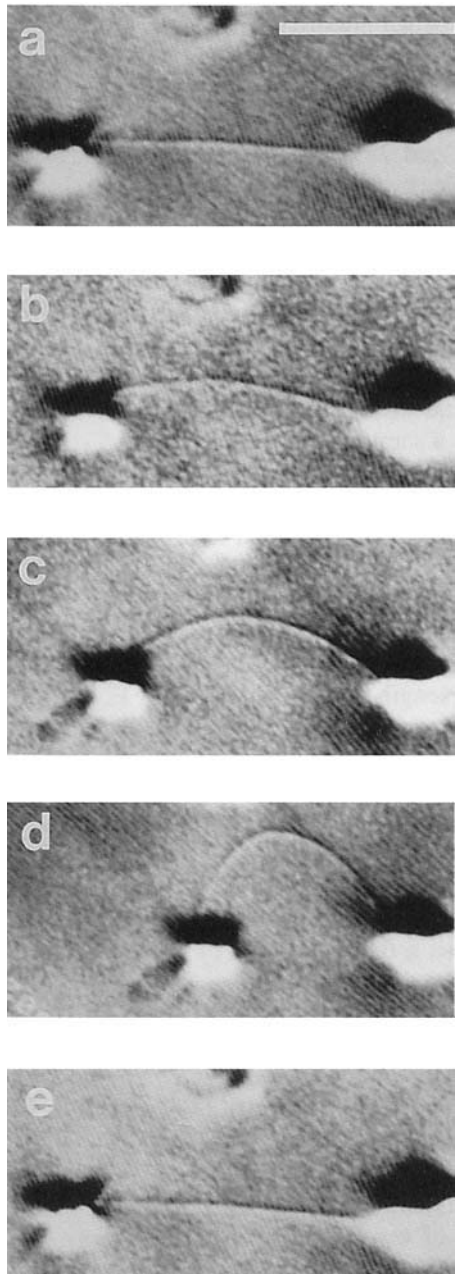

Fig. 4. Video-enhanced DIC images of a MAP-stabilized microtubule during a cycle of bending. **a:** A microtubule spontaneously stretched with one poly-L-lysine-coated glass microspheres attached at each end. The distance between two microspheres is 19.9 μm. The microsphere on the right end was attached to the inner surface of the coverglass and served as a hinged end. The other microsphere was held at around 2 μm below the glass surface with optical tweezers to prevent it from sticking to the glass. Since the focus is on the second microsphere, the one on the right is slightly out of focus. Concentration of microtubule-proteins was 0.5 mg/ml. Scale bar = 10 μm. **b:** Buckling was initiated by moving the optically trapped microsphere on the left. In this case, the critical load with which the microtubule started bending was 5 mW of laser power (corresponding to 1.5 pN). **c:** With increased trapping forces of 2.2 pN, the microtubule buckled until the limit to balance with the recovery force of microtubule. **d:** The microtubule was bent to the deflected length of 11.2 μm with a force of 2.9 pN. **e:** Beyond the bending limit in c or d, the microsphere escaped from the trap, and the microtubule recovered to the initial stretched condition.

TABLE I. Comparison of Flexural Rigidity Evaluated From Critical Load and Deflected Length Measurements*

Samples	Microtubule length (μm)	Critical load meas.		Deflected length meas.		
		Critical load (pN)	Flexural rigidity ($\times 10^{-23}$ Nm^2)	Force (pN)	Deflected length (μm)	Flexural rigidity ($\times 10^{-23}$ Nm^2)
MAP-stabilized microtubule	10.5	3.0	3.4	4.9	6.0	4.3
	10.5			3.7	9.1	3.8
	19.9	1.5	6.0	3.1	9.3	9.1
	27.9	1.5	12.0	3.3	17.0	20.0
Taxol-stabilized microtubule	4.4	0.7	0.13	1.2	3.6	0.20
	11.8	0.4	0.56	0.5	9.5	0.59

*Values are compared for MAP-stabilized and taxol-stabilized microtubules. Critical loads and deflected lengths are also listed.

Table I. As mentioned above, the critical load measurement contained possible experimental errors because the judgment of the initiation of deflection was difficult in some cases. (For example, appreciable difference in the critical load was not observed between microtubules 19.9 μm and 27.9 μm in length as shown in Table I.) Such difficulty was particularly significant for longer microtubules stabilized with taxol because the curvature fluctuated spontaneously.

Next we evaluated flexural rigidity from the deflected length x. These results are also summarized in Table I. Comparing the samples of the same lengths, the values evaluated from the deflection always are slightly higher than those evaluated from the critical load. For example, a sample with a length of 10.5 μm gave rigidity values of 4.3 $\times$ 10^{-23} Nm^2 and 3.8 $\times$ 10^{-23} Nm^2 from deflected length measurements, but a value of 3.4 $\times$ 10^{-23} Nm^2 was obtained from critical load measurement. For further confirmation, we checked deflected angles with the sample shown in Figure 4c,d. K(p) of 1.62 calculated from the measured deflected angle α = 39° in Figure 4c was identical with that measured from deflected length through Eq. (8). For Figure 4d, the difference becomes larger, probably owing to its asymmetric bending curvature. However, the difference in K(p) was within 6%. The flexural rigidity evaluated using both deflected angles and lengths agreed well (within 10%).

The flexural rigidities obtained from both the deflected length and critical load methods are plotted in Figure 5 as a function of filament length. Two conclusions can be drawn from these results: 1) MAP-stabilized microtubules are more rigid than taxol-stabilized microtubules, and 2) flexural rigidity depends on the microtubule length. For MAP-stabilized microtubules, EI increases 5 times, from 4 $\times$ 10^{-23} Nm^2 at 10 μm to 20 $\times$ 10^{-23} Nm^2 at 30 μm. Comparing the values at the same lengths of 10 μm, the flexural rigidity of MAP-stabilized microtubules (4 $\times$ 10^{-23} Nm^2) is about 4 times larger than that of taxol-stabilized microtubules (1 $\times$ 10^{-23} Nm^2).

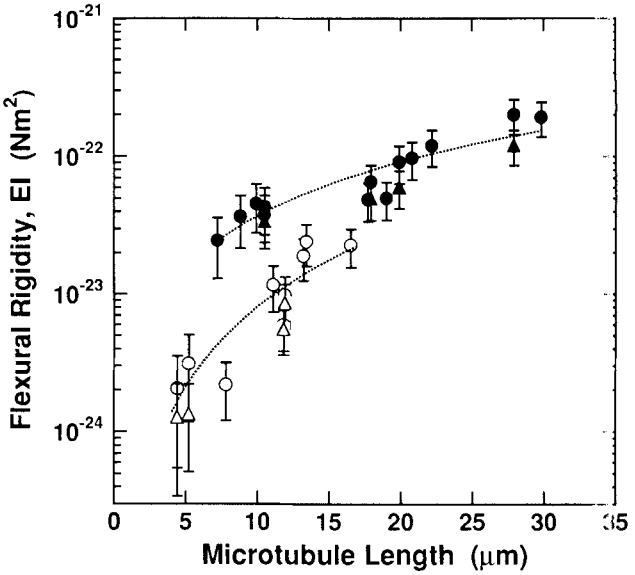

Fig. 5. Flexural rigidity of MAPs-stabilized microtubules (solid symbols) or taxol-stabilized microtubules (open symbols) plotted against microtubule length. Flexural rigidity was evaluated independently from the measurements of two different parameters, deflected length (circles) and critical load (triangles), which agreed reasonably well. Note the obvious length dependency of flexural rigidity in both types of microtubules. Curves obtained by least-squares fitting are also shown (see text).

DISCUSSION

Three ways of estimating flexural rigidity by microtubule buckling were compared and were shown to agree reasonably well. It was found that values obtained from critical load measurements tended to be slightly lower. Buckling through the attached microspheres is not purely compressive, but slight additional transverse force is applied before the start of bending. This may explain why the values obtained from critical load measurements are smaller.

Major errors in the measurements of flexural rigidity arise from two sources. One source is experimental errors in force and length evaluations. The other is the decline of the sample filament out of an ideal horizontal

focal plane of the microscope, as mentioned in the caption of Figure 4. Considering the laser power and force relation (0.3 ± 0.05 pN/mW) together with dispersion of microsphere sizes (1.6 ± 0.3 μm in diameter), the accuracy in the experimental evaluation of the compressing force is estimated to be $\Delta P/P = \pm 0.25$. Positions of both fixed and trapped microspheres were carefully measured with an accuracy of ±0.2 μm before compression, by adjusting the focus of their images separately. Since microtubules were not placed horizontally and the heights of the fixed and trapped microspheres differed by 2 μm, the trajected length should differ significantly from the true length. As a result, the combined errors in the length measurement increase for shorter samples, as $\Delta L = \pm 1.0$ μm for L = 5 μm and $\Delta L = \pm 0.5$ μm for L = 20 μm. Using the relation of $\Delta(EI)/EI = \Delta P/P + 2\Delta L/L$ for critical loads, $\Delta(EI)/EI$ is evaluated to be ±0.65 for 5 μm and ±0.30 for 20 μm. The declined angle also affects the direction of forces, but errors arising from force vectors are much smaller than those that are due to incorrect evaluation of lengths. Errors in shorter samples are more serious and critical than those in longer samples. It should be noted, however, that the difference in the flexural rigidity in shorter samples (around 5 μm) and in longer samples (around 20 μm) exceeds the evaluation errors.

Flexural rigidities for taxol-stabilized microtubules measured here by buckling agree well (within an order of magnitude) with those reported from thermal fluctuation measurements [Gittes et al., 1993] for taxol-stabilized samples but not so well with those obtained from bending curvature measurements [Mizushima-Sugano et al., 1983]. The latter may have underestimated the rigidity because MAP-stabilized microtubules stick easily to glass surfaces and their curvatures are modified. Precisely speaking, however, our values differ somewhat from those of Gittes et al. [1993]. Their values of 2.2×10^{-23} Nm^2 for taxol-stabilized microtubules with lengths between 25 and 65 μm are twice as high as those of 1.1×10^{-23} Nm^2 (averaged value) for taxol-stabilized microtubules with lengths of 4.4 to 16.5 μm. This difference may be mainly attributed to the length dependence of flexural rigidity, which was observed for the first time in our experiments. By extrapolating our data to lengths exceeding 30 μm, we can expect that the flexural rigidity increases to (4 to 6) $\times 10^{-23}$ Nm^2. The flexural rigidity of taxol-stabilized microtubules evaluated by Venier et al. [1994] was 0.47×10^{-23} Nm^2 for microtubules with lengths between 3 and 8 μm. This most recent value agrees well with ours (0.2 to 0.5 $\times 10^{-23}$ Nm^2; L = 5 to 8 μm from dotted line in Fig. 5) in this report. The fact that these three evaluations obtained independently by different methods yield values which agree well when length dependency is considered strongly suggests that the flexural rigidity of microtubules depends on length as we point out here for the first time.

Applying the moment of $I = 1.7 \times 10^{-32}$ m^4 (calculated for a cylinder with outer and inner diameters of 25 nm and 12.5 nm), Young's modulus for taxol-stabilized microtubules is nominally estimated to be 6×10^8 N/m^2 at around 10 μm in length. This value is similar to those of polyethylene (10^8 to 10^9 N/m^2) and polypropylene (10^9 to 10^{10} N/m^2). As observed in the previous works utilizing thermal fluctuations by Gittes et al. [1993] and Venier et al. [1994], the transverse force required to bend a filament is much smaller than the longitudinal compressing force. The critical transverse force can be described as $P_{tr} = 3EI\delta/L^3$ (δ: deflection), assuming one-fixed end and one-free end with a load to a rod of length L. Accordingly, the value of P_{tr} required to deflect a 20-μm-long filament of a microtubule is calculated to be 0.008 pN (for d = 2 μm, EI = 10^{-23} Nm^2), which is two orders of magnitude smaller than the critical longitudinal bending force. We chose to analyze longitudinal bending in our flexural rigidity measurements since such a small force is difficult to calibrate against thermal fluctuations in solution.

The direct buckling measurement revealed that the flexural rigidity EI is not a constant parameter defining the rigidity of a microtubule. Curves shown in Figure 5 indicate that the flexural rigidity of a taxol-stabilized microtubule increases in proportion to $L^{1.9}$, while that of a MAP-stabilized microtubule increases in proportion to $L^{1.3}$. Such deviation from the homogeneous rod assumption may be attributed to the specific helical nature existing in microtubules, owing to the twisting of protofilaments or spiral heaping of tubulin subunits. In particular, more than 80% of the MAP-stabilized microtubules used in our experiments are considered to be made of 14 protofilaments [Pierson et al., 1978], whereas filaments made of 12 protofilaments are the major (>50%) components for taxol-stabilized microtubules [Andreu et al., 1992]. Protofilaments in these microtubules are known to be twisted, unlike the straight stretched protofilaments in microtubules made of 13 protofilaments. According to the observation of microtubule rotation during kinesin movement, the pitch of such twisting in 14-protofilament microtubules is estimated to be 6.16 μm [Ray et al., 1993]. It is apparent that twisted or coiled structure deteriorates the homogeneous rod assumption used in the analysis and works to strengthen the flexural rigidity of a rod. In this sense, the three-dimensional superstructure that may exist in taxol-stabilized microtubules [Venier et al., 1994] will support the deviation of flexural rigidity analysis based on homogeneous rods. Another explanation is the absorption of compressing energy because the elastic model is based on the assumption that the change of rod length resulting from

compression is neglected. The increase of flexural rigidity with length means that the longitudinal force (P_{cr}) required to buckle a microtubule does not decrease in proportion to the square of length as expressed in Eq. (5), but remains almost constant as the filament grows, especially when assisted with taxol. This means that a microtubule is more resistant to longitudinal compressing forces than simply expected from homogeneous rod theory as it grows longer. Such a unique property of *microtubules* may be of critical importance to their biological activity, for example in supporting neurite outgrowth. We are now carrying out experiments to further analyze this length dependence together with the effects of MAPs on flexural rigidity.

ACKNOWLEDGMENTS

We thank T. Tashiro for critical reading of the manuscript, N. Sarukura for valuable advice, M. Kano for setting up the video-enhanced DIC microscope, and Y. Katsukura for technical assistance in the early stage of the work. One of the authors (M. Kurachi) was supported by the Special Researchers' Basic Science Program, Japan.

REFERENCES

Andreu, J.M., Bordas, J., Diaz, J.F., Garcia de Ancos, J., Gil, R., Medrano, F.J., Nogales, E., Pantos, E., and Towns-Andrews, E. (1992): Low resolution structure of microtubules in solution. Synchrotron X-ray scattering and electron microscopy of taxol-induced microtubules assembled from purified tubulin in comparison with glycerol and MAP-induced microtubules. J. Mol. Biol. 226:169–184.

Askin, A., and Dziedzic, J.M. (1987): Optical trapping and manipulation of viruses and bacteria. Science 235:1517–1520.

Bradford, M. (1976): A rapid and sensitive method for the quantitation of microgram quantities of protein utilizing the principle of protein-dye binding. Anal. Biochem. 72:248–254.

Dye, R.B., Fink, S.P., and Williams, R.C., Jr. (1993): Taxol-induced flexibility of microtubules and its reversal by MAP-2 and Tau. J. Biol. Chem. 268:6847–6850.

Edson, K., Weisshaar, B., and Matus, A. (1993): Actin depolymerisation induces process formation on MAP2-transfected non-neuronal cells. Development 117:689–700.

Feynman, R.P., Leighton, R.B., and Sands, M. (1964): "The Feynman Lectures on Physics," Vol. II. Reading, MA: Addison-Wesley.

Gittes, F., Mickey, B., Nettleton, J., and Howard, J. (1993): Flexural rigidity of microtubules and actin filaments measured from thermal fluctuations in shape. J. Cell Biol. 120:923–934.

Matus, A. (1994): Stiff microtubules and neuronal morphology. Trends Neurosci. 17:19–22.

Mizushima-Sugano, J., Maeda, T., and Miki-Noumura, T. (1983): Flexural rigidity of singlet microtubules estimated from statistical analysis of their contour lengths and end-to-end distances. Biochim. Biophys. Acta 755:257–262.

Pierson, G.B., Burton, P.R., and Himes, R.H. (1978): Alterations in number of protofilaments in microtubules assembled in vitro. J. Cell Biol. 76:223–228.

Ray, S., Meyhofer, E., Milligan, R.A., and Howard, J. (1993) Kinesin follows the microtubule's protofilament axis. J Cell Biol. 121:1083–1093.

Shelanski, M.L., Gaskin, F., and Cantor, C.R. (1973): Microtubule assembly in the absence of added nucleotides. Proc. Natl. Acad. Sci. U.S.A. 70:765–768.

Sloboda, R.D., Dentler, W.L., Bloodgood, R.A., Telzer, B.R., Granett, S., and Rosenbaum, J.L. (1976): Microtubule-associated proteins (MAPs) and the assembly of microtubules in vitro. In Goldman, R., Pollard, T., and Rosenbaum, J. (eds.): "Cell Motility." Cold Spring Harbor, NY: Cold Spring Harbor Laboratory, pp. 1171–1212.

Timoshenko, S.P., and Gere, J.M. (1961): "Theory of Elastic Stability," 2nd ed. New York: McGraw-Hill.

Venier, P., Maggs, A.C., Carlier, M.-F., Pantaloni, D. (1994): Analysis of microtubule rigidity using hydrodynamic flow and thermal fluctuations. J. Biol. Chem. 269:13353–13360.